associated to https://doi.org/10.1016/j.foodchem.2023.136636

Uncovering heterogeneity of anacardic acids from pistachio shells: a novel approach for structural characterization

Giovanni Ventura[1,2], Cosima Damiana Calvano[1,2], Davide Blasi[1], Davide Coniglio[1], Ilario Losito[1,2], Tommaso R.I. Cataldi[1,2]

[1] Department of Chemistry, [2]Interdepartmental Research Center SMART, University of Bari Aldo Moro, via Orabona 4, 70126, Bari, Italy

This is a pre-print version associated to paper with doi: 10.1016/j.foodchem.2023.136636

Number of Figures: 5

Number of Tables: 1

Supplementary material: yes

Keywords: Anacardic acids, pistachio shells, biomass, epoxidation, LC-MS/MS

Authors for correspondence, email: giovanni.ventura@uniba.it; tommaso.cataldi@uniba.it

Abstract

Anacardic acids (AnAs) are important secondary metabolites that occur primarily in plants of the *Anacardiaceae* family, such as pistachio (*Pistacia vera L.*). Some AnAs have been associated with health benefits, and the position of the C-C double bonds is a crucial feature of these metabolites. Herein, we propose a new strategy based on RPLC separation and detection by ESI-MS/MS, preceded by an epoxidation reaction. The procedure was applied to the green extracts of lignified pistachio shells, and a mixture of AnAs bearing alkyl chains 13:0, 15:0, and 17:1 emerged as prevailing. As positional isomers of AnA 15:1 (Δ^8 and Δ^6) and AnAs 17:1 (Δ^{10} and Δ^8) were identified for the first time, their discovery paves the way to the systematic study of their potential health-beneficial effects. The developed method was validated and applied to quantify AnAs in pistachio green extract, showing contents higher than 10 mg/ 100 g of biomass.

1. INTRODUCTION

The demand for bioactive compounds and natural antioxidants in human nutrition has increased considerably, leading to extensive research in this area (Mandalari et al., 2021).

Pistachios (*Pistacia vera* L.) are known to contain various bioactive compounds with diverse functions, such as anti-inflammatory, anticarcinogenic, antiangiogenic, antimicrobial, and antioxidant activities (Schulze-Kaysers et al., 2015). Studies focusing on the characterization of these compounds have shown the presence of phenolic lipids in both seed and outer pistachio hulls (Erşan et al., 2016; Grace et al., 2016; Saitta et al., 2009; Schulze-Kaysers et al., 2015).

Phenolic lipids structurally consist of a saturated or unsaturated (mono, bi- or tri-olefinic) hydrophobic alkyl chain linked to a modified phenolic group representing the hydrophilic head. Alkylphenolic acids, such as anacardic acids (AnAs), also belong to this class of compounds (Schulze-Kaysers et al., 2015). The term “anacardic acid” typically refers to a mixture of several closely related secondary metabolites, each consisting of a salicylic acid substituted with an alkyl chain. **Figure S1** shows the structures of some AnAs having 13, 15, and 17 carbon atoms on the side chains and zero, one or two unsaturations, respectively (*i.e.*, 2-hydroxy-6-tridecyl-benzoic acid, AnA 13:0, 2-hydroxy-6-pentadec-8-en-1-yl benzoic acid, AnA 15:1Δ^{8}, also known as *merulinic acid*, and 2-hydroxy-6-((8Z,11Z)-pentadeca-8,11-dien-1-yl) benzoic acid, AnA 17:2$\Delta^{8,11}$), with the numbering adopted in this work.

AnAs have been found to have a positive impact on human health; like fatty acids, they can reduce the incidence of cardiovascular diseases in individuals who consume a diet rich in fruits and vegetables (Arjeh et al., 2020). AnAs are natural phenols with high antioxidant activity (Gomes Júnior et al., 2020; Morais et al., 2017; Yalpani & Tyman, 1983). They also possess significant antibacterial properties (Chen et al., 2005; Himejima & Kubo, 1991; Kubo et al.,

1994; Muroi & Kubo, 1993) and have been shown to inhibit tumour cells, including those in pituitary adenoma (Gomes Júnior et al., 2020), prostate (Wu et al., 2011), pancreatic (Park et al., 2018), and breast (Q. Zhao et al., 2018) cancers. Interestingly, the health benefits of AnAs may be influenced by the number and position of unsaturations on the lateral alkyl chain (Kubo et al., 1993; Schulze-Kaysers et al., 2015), and the composition of AnA mixture varies depending on the plant species (Schulze-Kaysers et al., 2015).

So far, few studies have investigated the chemical composition of the lignified shells that cover the pistachio edible seeds (Yalpani & Tyman, 1983). Due to the ever-growing demand for shelled pistachios, large amounts of raw materials have become available. Hard shell powders of pistachio are mostly used as energy sources and/or raw materials for organic synthesis (Açıkalın et al., 2012). Additionally, both the hard and the soft shells of pistachio, once regarded as agricultural waste, can be utilized in the pharmaceutical industry upon the green extraction of active ingredients, including AnAs (Arjeh et al., 2020). The commonly accepted approach for AnAs characterization is based on gas chromatography (GC) and electron ionization (EI) mass spectrometry (MS) (Andrade et al., 2011; Gómez-Caravaca et al., 2010; Yalpani & Tyman, 1983). Very recently, the same GC-EI-MS approach was employed by Ohta et al. (Ohta et al., 2021) to study long-chain anacardic acid derivatives. However, a time-consuming derivatization procedure is necessary for the GC separation, which represents a disadvantage of this method. Conversely, research on the use of Cs^+ bombardment, a variant of fast atom bombardment (FAB), was reported by Claeys et al. in 1993 (Claeys et al., 1993) for the analysis of isolated AnAs from leaves and twigs of *Spondias mombin*. While this technique is fast, it results in a loss of species separation, which may be a drawback, especially in the case of the concurrent presence of isomers.

The present work contributes to a more comprehensive characterization of AnAs occurring in powdered hard shells of pistachio using a C30 column coupled with electrospray ionization and tandem mass spectrometry (ESI-MS/MS). Since structural differences of AnAs imply diverse health effects (Česla et al., 2006; Grace et al., 2016; Kubo et al., 1993; Rodrigues-Costa et al., 2020; Wu et al., 2011), an epoxidation reaction (Fringuelli et al., 1989), followed by tandem MS analysis, was also carried out to distinguish positional isomers of unsaturated AnAs. The proposed approach significantly simplified the characterization of this class of compounds, suggesting that tandem MS of epoxidized derivatives may be successfully exploited to investigate complex mixtures revealing novel and unexplored unsaturated AnAs. Notably, as the extract of pistachio shells contains AnAs, this suggests that phenolic lipids serve as important antioxidant species that can be recovered from these by-products. The method developed is suitable for the qualitative and quantitative analysis of AnAs, with limits of detection in the sub-micromolar range. Thus, the study aimed to provide a comprehensive view of the content of AnAs in this biomass.

2. MATERIALS AND METHODS

2.1 Chemicals. LC-MS grade water, acetonitrile, methanol (MeOH), hexane, chloroform ($CHCl_3$, HPLC grade), ammonium acetate (reagent grade), and meta-chloroperoxybenzoic acid (*m*-CPBA) were obtained from Sigma-Aldrich (Milan, Italy). Absolute ethanol (EtOH) was purchased from Panreact (99.8% vol). All anacardic acids were purchased from Sigma-Aldrich (Milan, Italy) and were used without further purification: AnA 13:0 (2-hydroxy-6-tridecyl-benzoic acid, $C_{20}H_{32}O_3$), AnA 15:0 (2-hydroxy-6-pentadecyl-benzoic acid or ginkgolic acid C15:0, $C_{22}H_{36}O_3$), AnA 15:1 (2-hydroxy-6-[(8Z)-pentadecenyl]-benzoic acid or ginkgolic acid C15:1, $C_{22}H_{34}O_3$), AnA 15:3 ≥85% (2-hydroxy-6-[(8Z,11Z,14)-pentadeca-8,11,14-trienyl]-

benzoic acid, $C_{22}H_{30}O_3$), and AnA 17:1 (2-hydroxy-6-[(10Z)-heptadecenyl]-benzoic acid or ginkgolic acid II C17:1, $C_{24}H_{38}O_3$).

2.2 Samples preparation and green extraction of phenolic lipids. Powders of pistachio shells (*Pistacia vera* cultivar *Napoletana*) were obtained by a procedure reported in the literature (Blasi et al., 2022). Dried shell fragments having a size smaller than 1 mm (obtained *via* hammer milling), were ball-milled–using a planetary micro mill Fritsch Pulverisette 7 (EMME3 srl, Milan, Italy) equipped with two stainless steel reactors of 12 mL.

Bronte pistachios (PDO) were acquired from a market in Sicily, and the dried shells were removed. 100 g of the shells were subjected to a prior hammer milling and the resulting biomass was filtered using a 1 mm sieve to achieve a suitable size for the ball-milling. Then, each reactor was loaded with approx. 2 g of biomass, together with 10 stainless steel spheres of 5 mm diameter, and 3 stainless steel spheres of 7 mm diameter. The milling process consisted of 8 cycles of 5 min at 450 rpm. After each cycle, a pause of 10 min was applied to limit the overheating of the biomass. The resulting powder was further sieved using a 0.5 mm sieve. To assess whether the ball milling pre-treatment and/or the Soxhlet extraction may trigger isomerization reactions, an aliquot of specimen was subjected to Soxhlet extraction soon after the sieving (thus without experiencing the pre-treatment), while another control specimen was obtained replacing the Soxhlet extraction with a simple maceration by stirring 10 mg of ball milled powder in 1 mL of ethanol at room temperature for 3 hours.

Ball-milled samples and non-ball-milled ones, both made up by 8.00 g of biomass, independently underwent a Soxhlet extraction for 12 hours using ethanol. The extract was dried to obtain a solid residue and weighed to determine the extraction yield being equal to 2.7 ± 0.3% on three replicates (Blasi et al., 2022). The three fractions were combined and

dissolved in ethanol, at a final concentration of 10 mg/mL. 1 mL of this solution was transferred into a vial, and slowly evaporated.

For lipid extraction, 10 mg of pistachio shell extract was dissolved in 2 mL of MeOH solution and left in an ultrasonic bath at 60 °C for 5 minutes, after which, the liquid phase was recovered, and 2 aliquots of 100 µL of the mixture were brought to dryness under N_2. One of the two aliquots was dissolved in 100 µL of the initial composition of the mobile phase and further diluted 1:50 using the same solution, ready to be injected into the LC-ESI-MS system, while the other was subjected to an epoxidation reaction.

2.3 Epoxidation of unsaturated lipids by *m*-CPBA. Epoxidation was performed using the Prilezhaev reaction, employing *m*-CPBA as an epoxidant agent and adapting the protocol reported by Coniglio *et al.* (Coniglio et al., 2022), where the reaction was used to identify the position of olefinic double bonds in arsenosugar-phospholipids (Coniglio et al., 2020). One of the two aliquots of the dried extract obtained from pistachio shells was dissolved in 100 µL of suspension of m-CPBA 2 mg/mL in $CHCl_3$. The epoxidation reaction was carried out at room temperature for 15 min; after incubation, 100 µL of H_2O was added to block epoxidation and the solution was dried under a gentle N_2 flow, and then resuspended in 100 µL of the initial composition of the mobile phase and diluted 1:50, ready to be injected into the LC-ESI-MS system. A standard solution of unsaturated AnAs was subjected to epoxidation by adding 100 µL of m-CPBA to 100 µL of the solution containing 20 ppm of each compound. The mixture was stirred for 15 minutes at room temperature before being diluted 1:50 with MeOH/H2O 60:40 (v/v). To estimate the reproducibility of the conversion yield, three analytical replicates were analysed.

2.4 Online identification of anacardic acids. In the commonly accepted nomenclature for lipids (Liebisch et al., 2013, 2017) the total number of carbon atoms and the total number of unsaturations are usually reported following an acronym representing lipid class. The same system was used here for anacardic acids (AnA), excluding from the calculation the carbon atoms and unsaturations of salicylic acid and referring to the lateral aliphatic chain (for example, 2-hydroxy-6-pentadecyl-benzoic acid is named AnA 15:0, since the alkyl chain contains 15 carbon atoms and no unsaturation). In the text, AnAs without side chain unsaturations are identified as "saturated". Conversely, for the unsaturated ones, the position of the olefinic double bond is indicated starting from the carbon atom linked to salicylic acid. For anacardic acids, entries (DB) obtained from the LipidMaps (Fahy et al., 2009) database were expanded by adding computational ones not yet present and expected *m/z* ratios after the epoxidation reaction. Measurements were carried out in triplicate and average values were calculated.

2.5 Instrumentation and operating conditions. Samples were analysed by using an Ultimate 3000 UHPLC system (Thermo Scientific, Waltham, MA, USA) coupled to a Velos Pro mass spectrometer (Thermo Scientific, Waltham, MA, USA), including a Linear Ion Trap analyser. The column effluent was transferred into the spectrometer through a heated electrospray ionization (HESI) interface. The main electrospray and ion optics parameters were the following: sheath gas flow rate, 35 arbitrary units (a.u.); auxiliary gas flow rate, 15 a.u.; spray voltage, -3.5 kV (negative polarity) and + 4.0 kV (positive polarity); capillary temperature, 320 °C; S-Lens RF Level, 60 a.u. The normalized collision energy (NCE) was set to 50% (in this case, a 400% value corresponds to a 100 V excitation voltage) using a 1 *m/z* unit-wide isolation window centred on the *m/z* ratio.

Accucore™ C30 RP-MS column (150 × 2.1 mm id, packed with 2.6 µm core-shell particles), equipped with the security guard cartridges (50 × 2.1 mm id), purchased from Thermo Scientific (Waltham, MA, USA) and operating at a flow rate of 0.20 mL/min was used to perform RPLC-ESI-MS experiments, working at 40 °C. The following binary elution program, based on water (solvent A) and methanol (solvent B), both containing 2.5 mM of ammonium acetate, was adopted: 0–10 min, isocratic at 60% solvent B; 10-50 min, linear gradient from 60 to 100% solvent B; 50-58 min, isocratic at 100% solvent B; 58–63 min, return to the initial composition, followed by a 5 min equilibration time. To assess the purity of commercially available AnA unsaturated standards, isocratic LC-ESI-MS analyses (80% solvent B) were carried out working.

2.6 Quantitative analysis

Calibration curves of AnAs were explored in the range 0.01–10.0 ppm by preparing standard mix solutions at six concentration levels (0.01, 0.05, 0.10, 0.50, 1.00 and 5.0 ppm each). Three injection replicates were considered. To evaluate the matrix effect, two pistachio extracts were spiked before analyses by adding AnA 15:3 at a concentration of 0.05 ppm and 0.50 ppm. Data were analysed in triplicate. Limits of detection (LOD) and quantification (LOQ) were respectively calculated as three- and ten-fold of the ratio between the standard deviation of the intercept and the slope of the calibration curves obtained in pure solvents.

3. RESULTS AND DISCUSSION

3.1 Separation and detection of anacardic acids (AnAs) by RPLC-ESI-MS

A typical example of the separation of two saturated, two monounsaturated and a polyunsaturated standard AnAs, i.e., 13:0 and 15:0, 15:1 and 17:1, and 15:3, obtained using an Accucore™ C30 column, is provided in plots A and B of **Figure S2**, respectively. Since the formation of deprotonated molecules (*i.e.*, $[M-H]^-$ ions) can be easily achieved, AnAs were effectively examined in ESI negative ion mode (Gómez-Caravaca et al., 2010). As expected, the retention behaviour of AnAs was affected by the chain length and unsaturation number, and the AnA 15:0 eluted later than AnAs 15:1 and 13:0. As for fatty acids, double bonds of the hydrocarbon side chain create much fewer flexible molecules, which are less retained on RP columns and therefore separated from their saturated counterparts. Thus, we studied the occurrence of AnAs in the Soxhlet ethanol green extract of dried pistachio shells, which were previously powdered by ball milling under mild conditions (see paragraph 2.2). Three multiple extracted ion current (EIC) chromatograms of the most important saturated, mono- and polyunsaturated AnAs are reported in **Figure 1**.

In plots A, B, and C are shown, respectively, the chromatographic profiles of deprotonated AnAs including alkyl chains 13:0 and 13:1, 15:0 and 15:1, and 17:0, 17:1, 17:2, and 17:3. Although the most abundant AnAs found in the shell extracts of *P. vera* were the AnAs 13:0, 15:0, and 17:1, the absolute content of AnAs 13:1 (*m/z* 317.2), 15:1 (*m/z* 345.2), 17:0 (*m/z* 375.3), 17:2 (*m/z* 371.3), and 17:3 (*m/z* 369.2) was not negligible. Relatively low-intensity peaks related to AnAs 19:0 and 19:1 were also observed. The occurrence of saturated and monounsaturated AnAs having 13, 15, and 17 carbon atoms in the alkyl chain in pistachio shells was already reported by Yalpani and co-workers in 1983 (Yalpani & H.P. Tyman, 1983) after NMR analysis. A complete list of AnAs identified in the present work is given in **Table 1**.

3.2 Multistage MS analysis of AnAs cannot locate the double bond position.

The ensuing tandem MS analysis by collisional-induced dissociation (CID) of available standard AnAs revealed product ions due to decarboxylated molecules $[M-CO_2-H]^-$ as the predominant peak. For instance, the MS/MS spectrum of AnA 15:1 at *m/z* 345.2 is shown in **Figure S3A**. Under the present experimental conditions, the position of double bonds on the hydrophobic alkyl chain of unsaturated AnAs cannot be established by tandem MS experiments. This is consistent with an earlier report (Rodrigues-Costa et al., 2020) concerning the identification of merulinic acid C (*i.e.*, AnA 17:1), which was recognised after dimethyl disulfide derivatization and GC-EI/MS analysis.

As reported in **Figure S3B**, also MS^3 analysis of decarboxylated species are not informative. CID-MS^3 spectrum of $[M-CO_2-H]^-$ ion at *m/z* 301.3 is dominated by two highly abundant peaks at *m/z* 106.0 and 119.1. The former corresponds to a radical anion formed most likely by homolytic cleavage of the C1'-C2' bond (*vide infra*), and was already reported by Jandera and coworkers (Česla et al., 2006). We observed 11 additional peaks ranging from *m/z* 133.1 to 273.2, with a 14.0 Da spacing (equivalent to CH_2 units). However, we were unable to determine the position of the double bond on the alkyl chain, as we did not find any marker fragments that would indicate its location.

The need for new strategies to determine the position of the double bond is highlighted in **Figure 2**. When the MS^3 spectra of the decarboxylated precursor ions of AnAs 17:0, 17:1, 17:2, and 17:3 identified in pistachio shell extracts were compared, no significant differences were noticed. Further, their tandem MS spectra (**Figure S4** and **Figure S5** in Supplementary material), as well as AnA 13:0, AnA 13:1, AnA 17:0, and AnA 19:0 evidenced only the common neutral loss of CO_2 in the gaseous phase.

In **Figure 2**, the common generation of the diagnostic radical ion $[C_7H_6O]^{-\bullet}$ at *m/z* 106.0 (Česla et al., 2006; Xing & Huan, 2022), and that of an even electron closely related product ion, $[C_7H_7O]^-$ at *m/z* 107.1, together with standards retention times, serves to confirm putative attributions. Despite the differences in signals' relative intensities in plots A, B, and C of **Figure 2**, rather similar sequences of product ions were attained. Lateral chain progressive fragmentation with consequent loss of methylene was achieved, yet no diagnostic signals of the olefinic double bond positions were distinguished. Finally, two series of ions, separated by 14.0 Da (*i.e.* single methylene groups $-CH_2-$) were observed in the MS/MS spectrum of the precursor ion at *m/z* 325.3 (see plot D), *i.e*. the decarboxylated ion of AnA 17:3, but no suitable information of the C=C positioning was inferred. To address this issue, an innovative method which involves epoxidation of AnAs was exploited and will be discussed in the next section.

3.3 Epoxidation of AnAs occurring in a green extracted sample of pistachio shells.

A detailed characterization of unsaturated AnAs implies the knowledge of the alkyl-chain length, the degree of unsaturation and the carbon-carbon double bond(s) location. To address this challenge, the Prilezhaev reaction (Prileschajew, 1909), which is one of the most common methods of *in vitro* epoxidation of alkenes using a common peroxyl acid (Hilker et al., 2001), was employed during the present study. An oxirane ring is a relatively "weaker chemical point" on the alkyl (or acyl) chain for CID activation, leading to bond cleavage and generating diagnostic fragment ions for the unambiguous establishment of the olefinic bond.

As reported in **Scheme S1**, the epoxidation occurs on each olefinic double bond of the alkyl chain, with a consequent increase of 16.0 Da multiples of the molecular weight. The epoxidation reaction was found to produce the desired oxidation effect with great selectivity, as illustrated in **Figure 3.** The intensities of saturated species do not vary significantly before

277 and after epoxidation, since the reaction does not occur on the benzene ring or the carboxyl
278 group, as illustrated in **Figure S6** (Supplementary material).
279 On the contrary, the intensities of unsaturated AnAs were greatly decreased; as an example,
280 the intensity of AnA 17:1 exhibited a 50-fold decrease upon 15 min of reaction. Concomitantly,
281 a few peaks related to the epoxidation process appeared in which the multiple EIC
282 chromatogram focused on the epoxidized forms of AnAs (*i.e.,* 13:1, 15:1 and 17:1) are shown
283 in plot A of **Figure 3**, while the EIC chromatograms of poly-epoxidized AnAs 17:2 and 17:3 are
284 reported in plot B. For comparison purposes, the same chromatographic conditions were
285 applied before and after the epoxidation. As expected, these reaction products, named epo-
286 AnAs, being more polar were less retained on the C30 stationary phase than their unmodified
287 counterparts, with retention times shifting almost proportional to the number of oxygens
288 inserted in the epoxidized species (compare **Figure 3** and **Figure 1**). Indeed, the epo-AnA 17:1
289 was almost 8 min less retained than AnA 17:1, and the epo^2-AnA 17:2 was ca. 17 min less
290 retained in comparison with AnA 17:2. Interestingly, after the epoxidation reaction, two
291 separate and distinct chromatographic peaks for the epo-AnA 15:1, respectively at 27.8 and
292 28.9 min, were observed. Similarly, a low-intensity signal slightly preceding the
293 chromatographic peak of AnA 17:1 was seen in the same chromatographic profile. This
294 observation was studied through a comparison of CID-MS/MS spectra of both isomeric species
295 (*vide infra*).
296 Finally, the epo^3-AnA 17:3 species was eluted at about 6 min, thus lowering the retention time
297 by ca. 30 min compared to its native precursor. In the following paragraphs, the CID-MS/MS
298 spectra of these epo-species will be discussed. Notably, the presence of two or three peaks
299 recognizable for epo-AnAs 17:2 and 17:3 could suggest the generation of more

diastereoisomeric species (see **Figure 3B**), yet no further attention was devoted to this issue at the present stage.

3.4 Tandem MS of epoxidized forms of monounsaturated AnAs of dried pistachio shells.

Figure 4A shows the CID-MS/MS spectrum of the precursor ion at *m/z* 389.3 of epo-AnA 17:1, which corresponds to the main chromatographic peak detected at 34.5 min in **Figure 3A**. The base peak (*m/z* 327.3) is attributable to the neutral loss of CO_2 along with a water molecule. Two diagnostic peak signals for the olefinic double bond location, exhibiting different intensities and spaced by 16 units, at *m/z* 219.1 and *m/z* 203.1, were obtained, thus suggesting the original compound as AnA 17:1Δ^8. Two different routes give rise to these product ions, which produce a terminal alkene and an aldehyde (Y. Zhao et al., 2017), respectively labelled as type "A_1" and "B_1" ions in **Scheme S2**, where the subscript number indicates that epoxidation occurred on the closest DB to the benzene ring. As gas-phase fragmentation occurs at the level of the oxirane ring, both these product ions are diagnostic for the location of the C-C double bond on the side chain. The employed labelling involves counting the number of carbon atoms of the latter from the benzene ring. In this case, the product ions at *m/z* 219.1 and *m/z* 203.1 testify that the double bond is located between carbons 8 and 9 of the side chain, thus the AnA corresponds to a 2-hydroxy-6-(8)-heptadecenyl-benzoic acid. As a rule, the first sp^2 C atom on the lateral chain of an unsaturated AnA (y) can be easily determined by using the following empirical formula:

$$y = \frac{x' - 92 - 16 + 1}{14} = \frac{x'' - 92 + 1}{14}$$

where x' and x'' are the nominal masses due to peak signals of the aldehyde and alkene product ions, and 16, 1, and 14 are nominal masses of O, H, and CH_2, respectively. For all AnAs

studied, the alkene product ion (type A) exhibited a lower abundance than the aldehyde (type B) one, which was sometimes hardly detectable if it is observed at all. For instance, for the case discussed above where x'=219 and x''=203, the position of the first C involved in the double bond is y=8.

The CID-MS/MS spectrum underlying the chromatographic peak of AnA 17:1 at 33.9 min is reported in **Figure 4B**. Product ions detected at *m/z* 247.2 and *m/z* 231.2 revealed the occurrence of a relatively low peak signal of 2-hydroxy-6-(heptadic-10-en-1-yl) benzoic acid or AnA 17:1Δ^{10}. In the examined dried pistachio shells, peak signals of AnA 17:1 Δ^8/Δ^{10} positional isomers were in an approximately 20:1 ratio. The retention time data of monounsaturated epo-AnAs indicates that compounds with the epoxide closer to the polar head have a greater retention time. The epo-AnA 15:1Δ^6 exhibited a retention time greater than that of its isomer Δ^8, and the epo-AnA 17:1Δ^{10} presented a retention time slightly lower than the Δ^8 positional isomer, agreeing with retention dominated by the chain length and double bond position of the epo-species.

To verify the above discovery, we applied the same reasoning to product ions of both isomers of epo-AnA 15:1, using the CID-MS/MS spectra for the precursor ion at *m/z* 361.2 (plots C and D of **Figure 4**) averaged under the chromatographic peaks at 27.8 and 28.9 min. In both cases, the most intense ions are due to the loss of CO_2 (*m/z* 317.2) along with its dehydrated derivate (*m/z* 299.2). The main differences are due to diagnostic ions of the different C=C positions. The more abundant isomer, eluting at 27.8 min, has product ions at *m/z* 219.1 and *m/z* 203.1 that allowed us to locate the unsaturation at carbons 8' and 9', corresponding to AnA 15:1Δ^8. For the less abundant positional isomer that eluted later, product ions at *m/z* 191.1 and *m/z* 175.1 revealed that the olefinic double bond is located between C6' and C7' (see **Table 1**). Intriguingly, 2-hydroxy-6-(pentadic-8-en-1-yl) benzoic acid (*i.e.*, AnA 15:1Δ^8) and 2-hydroxy-6-

(pentadic-6-en-1-yl) benzoic acid (i.e., AnA 15:1Δ^6) coexist in the sample. It is interesting to note that the latter has been never reported by any source, including the LipidMAPS database. Other tandem MS spectra of epo-AnAs 13:1 and 19:1 are given in plots A and B of **Figure S7** (Supplementary material). Again, peak signals detected at *m/z* 247.2 and *m/z* 231.2 revealed the occurrence of a double bond between C10' and C11' of AnA 19:1 (thus corresponding to AnA 19:1Δ^{10}). When the epo-AnA 13:1 was fragmented, only the terminal alkene product ion was observed at *m/z* 147.1. Despite this, the peak signal revealed that the unsaturation was located between C4' and C5' of the lateral acyl chain, thus leading to AnA 13:1Δ^4. Note that diagnostic product ions of AnAs at *m/z* 106.0, 107.1 and 119.1, were not observed in the CID-MS/MS product ion spectra of epo-AnAs (see **Figure 4**). Overall, the epoxidation reaction appears rather easy, with a nearly complete conversion of the unsaturated species to the corresponding epo-AnAs. **Figure S7** (Supplementary material) illustrates the multiple-EIC chromatograms of unreacted AnAs occurring in the pistachio shell extracts after the epoxidation reaction.

To verify that the occurring compounds did not arise as artefacts of the proposed method, including ball-milling, Soxhlet extraction, and epoxidation, a reaction was carried out on two additional samples that were respectively obtained from (i) hammer milling and Soxhlet extraction (Blasi et al., 2022) or (ii) ball milling coupled with a room-temperature maceration in EtOH. As reported in **Figure S8**, only slight variations in the signal intensity were observed, and they are most likely due to the overall extraction yield. As for the derivatization using *m*-CPBA, even though in other lipid classes the epoxidation did not cause the migration of double bonds (Zhao et al., 2017; Coniglio et al., 2022), standard solutions of monounsaturated AnAs were derivatized to exclude the occurrence of isomerization reactions. Despite obtaining two peaks in the chromatographic traces acquired on AnA 17:1 epoxidized (**Figure S9**A), there was

no evidence about the onset of side reactions, since the isocratic elution of a standard solution of AnA 17:1 before epoxidation (see Figure **S9B**) revealed the occurrence of two peaks, thus indicating that the standard compound was rather a mixture of two AnAs 17:1 isomers.

3.5 Tandem MS of epoxidized derivatives of polyunsaturated AnAs.

To further verify the capability to assess double C-C bond locations of AnAs through the MS/MS analysis of their epoxidized forms and to characterize the AnAs of pistachio shells, some polyunsaturated AnAs containing two and three double bonds were investigated (**Figure S10**). The analysis of unknown poly-epoxidized compounds was more difficult because a plethora of peaks appeared in the tandem MS spectra due to multiple bond cleavages. A possible strategy to overcome this complication might be the epoxidation of a single double bond at a time and the ensuing investigation by MS/MS, applying the above-illustrated rules (Y. Zhao et al., 2017). However, this method requires knowledge of the lipid concentrations and reaction kinetics, and it does not apply to complex mixtures.

Herein, we analyzed the MS/MS spectrum of a standard triply epoxidized AnA, used as a model compound, for the complete identification of product ions. To this aim, 2-hydroxy-6-(8Z,11Z,14-pentadecatrien-1-yl-benzoic acid (*i.e.*, AnA 15:3 $\Delta^{8Z,11Z,14}$), available as an authentic standard, was epoxidized and then examined by MS and MS/MS. As expected, a peak at *m/z* 389.2 ($[epo^3\text{-}M-H]^-$) of a triply epoxidized species was obtained in the MS spectrum averaged under the corresponding chromatographic peak. The tandem MS spectrum of the species is reported in **Figure S10A.** Two not informative peaks were obtained at *m/z* > 300, *i.e.*, peaks at *m/z* 327.2 and 309.2, due, respectively, to CO_2 gas-phase loss followed by that of one and two water molecules. These product ions confirmed that water loss from the oxirane ring is a rather common process, especially when dealing with poly-epoxidized species. The two

already discussed peaks at *m/z* 203.1 and *m/z* 219.1 (*i.e.*, A_1 and B_1 type ions, see **Scheme S2**), diagnostic of the Δ^8 unsaturation, were detected. Expected A_2 type ions were found at *m/z* 259.2, while B_2 ones, at *m/z* 275.2, were not present, but an intense peak at *m/z* 257.2, recognised as B_2-H_2O, was found and can be deemed diagnostic of a C=C Δ^{11} unsaturation. It should be noted that, although the number of fragments does increase the spectral congestion, the CID-MS/MS of epo-AnA 15:3 was still interpreted based on product ions described in **Figure 5**, which include further epoxidation-related product ions, labelled as C_x-type ions (*i.e.* C_1 at *m/z* 233.2) and D_x-type ions (D_1 at *m/z* 247.2). Importantly, the intact oxirane rings in structures C and D give rise to these product ions.

The product ions *A*, *B*, *C*, and *D*, along with their closely related fragments, can be computed easily by their corresponding *m/z* values. These ions are labelled based on the previously defined nomenclature. The first and second double bonds of the AnA 15:3 reference compound were recognised as $\Delta^{8,11}$, and, despite the third double bound is located at the terminal end of the alkyl chain, diagnostic peak signals in the CID-MS/MS spectra were attained. Indeed, the product ions at 297.3 (A_3-H_2O) confirmed that the third double bond is positioned among C14' and C15'.

After assessing the possibility of locating multiple C=C bonds of AnAs through epoxidation, we investigated the unsaturated species recognised in the green extracted sample of dried and powdered pistachio shells (see **Table 1**). Both shorthand nomenclatures of AnAs, i.e. Δ and ω, were inserted for comparative studies.

Figure S10B shows the CID-MS/MS spectrum of a species recognized as epo^2-AnA 17:2, detected at *m/z* 403.2, which was found in the powdered sample of pistachio shells. Compared with the epo^3-AnA 15:3, a similar fragmentation behaviour was attained as the base peak was due to the loss of CO_2 and water (*m/z* 341.2). Accordingly, a further loss of H_2O explains the

formation of the peak signal at *m/z* 323.2. The product ions at *m/z* 219.1 and *m/z* 203.1 were diagnostic of the first olefinic position located between the C8' and C9'. A relatively intense A_2-type ion, detected at *m/z* 259.2, revealed that the second double bond is situated among C11' and C12'. Indeed, while the B_2-type ion at *m/z* 275.2 was found to be negligible, as in the case of AnA 15:3, the double bond position was confirmed by two distinctive ions generated by a further water loss, *i.e.*, $[A_2-H_2O]^-$ at *m/z* 241.2 and $[B_2-H_2O]^-$ at *m/z* 257.2. Therefore, the unsaturated AnA was identified as $17{:}2\Delta^{8,11}$, with isolated double bonds that behave similarly to a molecule containing only one double bond.

An illustrative example of the CID-MS/MS spectrum of the epo^3-AnA 17:3 (*m/z* 417.3) is reported in **Figure S10C**. The tandem MS spectrum resembles that of the epoxidized form of standard AnA 15:3. Ions at *m/z* 203.1, and 219.1 (A_1 and B_1, respectively) enabled us to determine the Δ^8 position as the first unsaturation, and B_2-H_2O was diagnostic of the Δ^{11} unsaturation. Finally, the already discussed product ion at *m/z* 297.3 (A_3-H_2O) was an important clue for the location of the third double bond between C14' and C15'. As a result, the triply unsaturated AnA 17:3 occurring in the dried pistachio shells was recognised as $\Delta^{8,11,14}$. We wish to emphasize that collectively the ω^9 family in the extracted sample of pistachio shells was the most expressed population of these plant secondary metabolites. The consequences of such an intriguing biosynthetic pathway deserve further investigation (Ohta et al., 2021).

Based on the results discussed so far, a pair of product ions related to epoxidized derivatives can be combined to uniquely identify the position of double bonds in unsaturated AnAs. This strategy has the advantage of distinguishing the C-C double location along the fatty alkyl chain without a reference compound. Furthermore, it is possible to develop algorithms that automatically identify the diagnostic product ions of epoxidated AnAs obtained by CID tandem

MS, which have predictable *m/z* values, similar to other lipids. The separation of epoxidized isomeric species, using a C30 RP column, was found an invaluable means to recognise all unsaturated AnAs occurring in the extracted samples of pistachio by-products. Work is underway to expand the present approach to other by-products of the *Anacardiaceae* plant family.

3.6 Quantification of anacardic acids

To establish linearity, limits of detection (LOD), and limits of quantification (LOQ) for each AnA, both spiked samples and standard solutions were examined. Since AnA 15:3 was not detected in the investigated specimens, the matrix effect was evaluated using spiked samples, which were prepared by adding a standard solution of AnA 15:3 at the concentration of 0.05 and 0.50 ppm. A comparison of EIC areas of AnA 15:3 in spiked and standard solution samples indicated that the matrix effect was negligible, since ratio among EIC areas is lower than 10%. **Table S1** and **Figure S11** (Supplementary Material) summarize the linear calibration data obtained for standard solutions dissolved in methanol/water 60:40 (v/v). The sub-micromolar range of limits of detection (LODs) for AnA 13:0, AnA 15:0, AnA 15:1, AnA 15:3, and AnA 17:1 were 0.050, 0.037, 0.032, 0.047, and 0.040 μM, respectively. The choice of the concentrations range used to make the calibration curves was based on the ionization properties of AnAs. The formation of a bis-deprotonated sodiated dimer, $[2M-2H+Na]^{-}$, even at concentrations as low as 0.5 ppm was observed. Its identity was confirmed by its tandem mass spectrum. However, the area of the dimer did not exceed 10% of that of the monomer even when injecting solutions at a concentration of 1 ppm. To account for this effect, the calibration curves were constructed by summing the areas of both dimer and monomer ions. Additionally, the samples were greatly diluted for accurate quantification. It is important to note that the ionization yields of AnAs vary due to the increase in the mobile phase of the methanol content, the

different lengths of acyl chains, and the presence of double bonds, as shown in **Figure S2**. Such an RPLC-ESI-MS chromatogram was obtained by injecting all the standards at a final concentration of 1 ppm each. The calibration curve for AnA 17:1 was used to quantify all other AnAs with 17 carbon atoms, while AnA 13:0 was used to compute the concentration of AnA 13:1. The quantitative results, presented in **Table S2**, represent the mean of three replicates ± standard deviation, reported in µM for the injected samples and mg AnA/100 g biomass. The analyzed samples contained approximately 3.4 (± 0.9) mg of AnA 13:0 and 3.5 (± 0.5) mg of AnA 17:1, corresponding to an aggregate content of approximately 7 mg/100 g of dry pistachio shells.

CONCLUSIONS

To our knowledge, this is the first work that describes the LC separation and MS detection of AnAs after a green extraction ~~ed~~ from hard shell powders of pistachio samples. An effective chromatographic setup based on a C30 column was developed to separate monounsaturated AnAs as epoxidized species since their derivatization was a key to pursuing their separation. Indeed, the *in vitro* epoxidation reaction led to both distinguishing AnAs differing in the DB position and pinpointing C=C bonds along polyunsaturated chains by the acquisition of tandem mass spectra. Such achievements can be considered as the starting point to develop strategies for the isolation of AnAs to better understand their biological roles. The significance of the present results can be applied to other samples including compounds possessing unsaturated alkyl chains, whether they belong to the AnA class or not.. Although lignified pistachio shells are currently considered by-products with low economic value, the present work has shown that they are a valuable source of AnAs, including unsaturated ones, which

can be responsible for desirable health properties, since concentrations of monounsaturated and saturated AnAs exceeding 6 and 5 mg per 100 g of lignified biomass, respectively, were found. Work is currently underway to optimize the extractive conditions for the biomass valorization process, including the solvent composition, temperature, time, and technique, as these factors can significantly affect the process.

ACKNOWLEDGMENTS

GV gratefully acknowledges PON Ricerca E Innovazione 2014-2020 – Azione IV.6 “Contratti di ricerca su tematiche Green” - Progects DM 1062. This work was supported by the project PONa3_00395/1 “BIOSCIENZE & SALUTE (B&H)” of Italian Ministero per l'Istruzione, l'Università e la Ricerca (MIUR). DB gratefully acknowledges the REFIN (Return for Future Innovation) action for funding, an initiative co-funded by European Union through the POR Puglia 2014–2020 (ID grant 2455F798).

Author Contributions

G.V.: conceptualization, methodology, writing− original draft preparation; C.D.C. supervision, writing−original draft preparation; D.B.: Samples preparation; D.C.: methodology; I.L: writing−reviewing and editing; T.R.I.C.: writing−reviewing and editing, funding acquisition, resources.

REFERENCES

Açıkalın, K., Karaca, F., & Bolat, E. (2012). Pyrolysis of pistachio shell: Effects of pyrolysis conditions and analysis of products. *Fuel*, *95*, 169–177. https://doi.org/10.1016/j.fuel.2011.09.037

Andrade, T. D. J. A. D. S., Araújo, B. Q., Citó, A. M. D. G. L., Da Silva, J., Saffi, J., Richter, M. F., & Ferraz, A. D. B. F. (2011). Antioxidant properties and chemical composition of technical Cashew Nut Shell Liquid (tCNSL). *Food Chemistry*, *126*(3), 1044–1048. https://doi.org/10.1016/j.foodchem.2010.11.122

Arjeh, E., Akhavan, H.-R., Barzegar, M., & Carbonell-Barrachina, Á. A. (2020). Bio-active compounds and functional properties of pistachio hull: A review. *Trends in Food Science & Technology*, *97*, 55–64. https://doi.org/10.1016/j.tifs.2019.12.031

Blasi, D., Mesto, D., Cotugno, P., Calvano, C. D., Lo Presti, M., & Farinola, G. M. (2022). Revealing the effects of the ball milling pretreatment on the ethanosolv fractionation of lignin from walnut and pistachio shells. *Green Chemistry Letters and Reviews*, *15*(4), 893–902. https://doi.org/10.1080/17518253.2022.2143244

Borenstein, R., Hanson, B. A., Markosyan, R. M., Gallo, E. S., Narasipura, S. D., Bhutta, M., Shechter, O., Lurain, N. S., Cohen, F. S., Al-Harthi, L., & Nicholson, D. A. (2020). Ginkgolic acid inhibits fusion of enveloped viruses. *Scientific Reports*, *10*(1), 1–12. https://doi.org/10.1038/s41598-020-61700-0

Česla, P., Blomberg, L., Hamberg, M., & Jandera, P. (2006). Characterization of anacardic acids by micellar electrokinetic chromatography and mass spectrometry. *Journal of Chromatography A*, *1115*(1–2), 253–259. https://doi.org/10.1016/j.chroma.2006.02.070

Chen, L., Cheng, X., Shi, W., Lu, Q., Go, V. L., Heber, D., & Ma, L. (2005). Inhibition of Growth of Streptococcus mutans , Methicillin-Resistant Staphylococcus aureus , and Vancomycin-Resistant Enterococci by Kurarinone, a Bioactive Flavonoid Isolated from Sophora flavescens. *Journal of Clinical Microbiology*, *43*(7), 3574–3575. https://doi.org/10.1128/JCM.43.7.3574-3575.2005

Claeys, M., van den Heuvel, H., Claereboudt, J., Corthout, J., Pieters, L., & Vlietinck, A. J. (1993). Determination of the double bond position in long-chain 6-alkenyl salicylic acids by collisional activation. *Biological Mass Spectrometry*, *22*(11), 647–653. https://doi.org/10.1002/bms.1200221105

Coniglio, D., Calvano, C. D., Ventura, G., Losito, I., & Cataldi, T. R. I. (2020). Arsenosugar Phospholipids (As-PL) in Edible Marine Algae: An Interplay between Liquid Chromatography with Electrospray Ionization Multistage Mass Spectrometry and Phospholipases A1 and A2 for Regiochemical Assignment. *Journal of the American Society for Mass Spectrometry*, *31*(6), 1260–1270. https://doi.org/10.1021/jasms.0c00094

Coniglio, D., Ventura, G., Calvano, C. D., Losito, I., & Cataldi, T. R. I. (2022). Positional Assignment of C−C Double Bonds in Fatty Acyl Chains of Intact Arsenosugar Phospholipids Occurring in Seaweed Extracts by Epoxidation Reactions. *Journal of the American Society for Mass Spectrometry*, *33*(5), 823–831. https://doi.org/10.1021/jasms.2c00006

Erşan, S., Güçlü Üstündağ, Ö., Carle, R., & Schweiggert, R. M. (2016). Identification of phenolic compounds in red and green pistachio (Pistacia vera l.) hulls (exo- and mesocarp) by HPLC-DAD-ESI-(HR)-MSn. *Journal of Agricultural and Food Chemistry*, *64*(26), 5334–5344. https://doi.org/10.1021/acs.jafc.6b01745

Fahy, E., Subramaniam, S., Murphy, R. C., Nishijima, M., Raetz, C. R. H., Shimizu, T., Spener, F., Van Meer, G., Wakelam, M. J. O., & Dennis, E. A. (2009). Update of the LIPID MAPS comprehensive classification system for lipids. *Journal of Lipid Research*, *50*(SUPPL.), 9–14. https://doi.org/10.1194/jlr.R800095-JLR200

Fringuelli, F., Germani, R., Pizzo, F., & Savelli, G. (1989). Epoxidation reaction with m-chloroperoxybenzoic acid in water. *Tetrahedron Letters*, *30*(11), 1427–1428. https://doi.org/10.1016/S0040-4039(00)99483-8

Gomes Júnior, A. L., Islam, M. T., Nicolau, L. A. D., de Souza, L. K. M., Araújo, T. de S. L., Lopes de Oliveira, G. A., de Melo Nogueira, K., da Silva Lopes, L., Medeiros, J.-V. R., Mubarak, M. S., & Melo-Cavalcante, A. A. de C. (2020). Anti-Inflammatory, Antinociceptive, and Antioxidant Properties of Anacardic Acid in Experimental Models. *ACS Omega*, *5*(31), 19506–19515. https://doi.org/10.1021/acsomega.0c01775

Gómez-Caravaca, A. M., Verardo, V., & Caboni, M. F. (2010). Chromatographic techniques for the determination of alkyl-phenols, tocopherols and other minor polar compounds in raw and roasted cold pressed cashew nut oils. *Journal of Chromatography A*, *1217*(47), 7411–7417. https://doi.org/https://doi.org/10.1016/j.chroma.2010.09.054

Grace, M. H., Esposito, D., Timmers, M. A., Xiong, J., Yousef, G., Komarnytsky, S., & Lila, M. A.

(2016). Chemical composition, antioxidant and anti-inflammatory properties of pistachio hull extracts. In *Food Chemistry* (Vol. 210, pp. 85–95). https://doi.org/10.1016/j.foodchem.2016.04.088

Hilker, I., Bothe, D., Prüss, J., & Warnecke, H.-J. (2001). Chemo-enzymatic epoxidation of unsaturated plant oils. *Chemical Engineering Science*, *56*(2), 427–432. https://doi.org/10.1016/S0009-2509(00)00245-1

Himejima, M., & Kubo, I. (1991). Antibacterial agents from the cashew Anacardium occidentale (Anacardiaceae) nut shell oil. *Journal of Agricultural and Food Chemistry*, *39*(2), 418–421. https://doi.org/10.1021/jf00002a039

Kubo, I., Muroi, H., Himejima, M., Yamagiwa, Y., Mera, H., Tokushima, K., Ohta, S., & Kamikawa, T. (1993). Structure-antibacterial activity relationships of anacardic acids. *Journal of Agricultural and Food Chemistry*, *41*(6), 1016–1019. https://doi.org/10.1021/jf00030a036

Kubo, I., Muroi, H., & Kubo, A. (1994). Naturally Occurring Antiacne Agents. *Journal of Natural Products*, *57*(1), 9–17. https://doi.org/10.1021/np50103a002

Liebisch, G., Ekroos, K., Hermansson, M., & Ejsing, C. S. (2017). Reporting of lipidomics data should be standardized. *Biochimica et Biophysica Acta - Molecular and Cell Biology of Lipids*, *1862*(8), 747–751. https://doi.org/10.1016/j.bbalip.2017.02.013

Liebisch, G., Vizcaíno, J. A., Köfeler, H., Trötzmüller, M., Griffiths, W. J., Schmitz, G., Spener, F., Wakelam, M. J. O., Vizcaino, J. A., Kofeler, H., Trotzmuller, M., Griffiths, W. J., Schmitz, G., Spener, F., & Wakelam, M. J. O. (2013). Shorthand notation for lipid structures derived from mass spectrometry. *The Journal of Lipid Research*, *54*(6), 1523–1530. https://doi.org/10.1194/jlr.M033506

Mandalari, G., Barreca, D., Gervasi, T., Roussell, M. A., Klein, B., Feeney, M. J., & Carughi, A. (2021). Pistachio Nuts (Pistacia vera L.): Production, Nutrients, Bioactives and Novel Health Effects. *Plants*, *11*(1), 18. https://doi.org/10.3390/plants11010018

Morais, S., Silva, K., Araujo, H., Vieira, I., Alves, D., Fontenelle, R., & Silva, A. (2017). Anacardic Acid Constituents from Cashew Nut Shell Liquid: NMR Characterization and the Effect of Unsaturation on Its Biological Activities. *Pharmaceuticals*, *10*(4), 31. https://doi.org/10.3390/ph10010031

Muroi, H., & Kubo, I. (1993). Bactericidal activity of anacardic acids against Streptococcus mutans and their potentiation. *Journal of Agricultural and Food Chemistry*, *41*(10),

1780–1783. https://doi.org/10.1021/jf00034a049

Ohta, S., Takeda, M., Ohta, E., Nehira, T., Ômura, H., Uy, M. M., & Ishihara, Y. (2021). Janohigenins: Long-chain anacardic acid derivatives with neuroprotective activity from Ophiopogon japonicus seeds. *Phytochemistry*, *191*, 112904. https://doi.org/10.1016/j.phytochem.2021.112904

Park, M., Upton, D., Blackmon, M., Dixon, V., Craver, S., Neal, D., & Perkins, D. (2018). Anacardic acid inhibits pancreatic cancer cell growth, and potentiates chemotherapeutic effect by Chmp1A - ATM - p53 signaling pathway. *BMC Complementary and Alternative Medicine*, *18*(1), 71. https://doi.org/10.1186/s12906-018-2139-3

Prileschajew, N. (1909). Oxydation ungesättigter Verbindungen mittels organischer Superoxyde. *Berichte Der Deutschen Chemischen Gesellschaft*, *42*(4), 4811–4815. https://doi.org/10.1002/cber.190904204100

Rodrigues-Costa, F., Slivinski, J., Ióca, L. P., Bertonha, A. F., de Felício, R., Cunha, M. G. da, da Mata Madeira, P. V., Cauz, A. C. G., Trindade, D. M., Freire, V. F., Ropke, C. D., Gales, A., Brocchi, M., Ferreira, A. G., Gueiros-Filho, F., Trivella, D. B. B., Berlinck, R. G. S., & Dessen, A. (2020). Merulinic acid C overcomes gentamicin resistance in Enterococcus faecium. *Bioorganic Chemistry*, *100*(May), 103921. https://doi.org/10.1016/j.bioorg.2020.103921

Saitta, M., Giuffrida, D., La Torre, G. L., Potortì, A. G., & Dugo, G. (2009). Characterisation of alkylphenols in pistachio (Pistacia vera L.) kernels. In *Food Chemistry* (Vol. 117, Issue 3, pp. 451–455). https://doi.org/10.1016/j.foodchem.2009.04.043

Schulze-Kaysers, N., Feuereisen, M. M., & Schieber, A. (2015). Phenolic compounds in edible species of the Anacardiaceae family – a review. *RSC Advances*, *5*(89), 73301–73314. https://doi.org/10.1039/C5RA11746A

Wu, Y., He, L., Zhang, L., Chen, J., Yi, Z., Zhang, J., Liu, M., & Pang, X. (2011). Anacardic Acid (6-Pentadecylsalicylic Acid) Inhibits Tumor Angiogenesis by Targeting Src/FAK/Rho GTPases Signaling Pathway. *Journal of Pharmacology and Experimental Therapeutics*, *339*(2), 403–411. https://doi.org/10.1124/jpet.111.181891

Xing, S., & Huan, T. (2022). Radical fragment ions in collision-induced dissociation-based tandem mass spectrometry. *Analytica Chimica Acta*, *1200*, 339613. https://doi.org/10.1016/j.aca.2022.339613

Yalpani, M., & H.P. Tyman, J. (1983). The phenolic acids of Pistachia vera. *Phytochemistry*, *22*(10), 2263–2266. https://doi.org/10.1016/S0031-9422(00)80158-2

Zhao, Q., Zhang, X., Cai, H., Zhang, P., Kong, D., Ge, X., Du, M., Liang, R., & Dong, W. (2018). Anticancer effects of plant derived Anacardic acid on human breast cancer MDA-MB-231 cells. *American Journal of Translational Research*, *10*(8), 2424–2434. http://www.ncbi.nlm.nih.gov/pubmed/30210681

Zhao, Y., Zhao, H., Zhao, X., Jia, J., Ma, Q., Zhang, S., Zhang, X., Chiba, H., Hui, S.-P., & Ma, X. (2017). Identification and Quantitation of C═C Location Isomers of Unsaturated Fatty Acids by Epoxidation Reaction and Tandem Mass Spectrometry. *Analytical Chemistry*, *89*(19), 10270–10278. https://doi.org/10.1021/acs.analchem.7b01870

Table 1**.** List of saturated and unsaturated (mono-, di-, or triply unsaturated) anacardic acids (AnAs) identified in the dried and hard shell of pistachio (*Pistacia vera* cultivar *Napoletana*) samples. [a]

N.	AnA [b]	RT (min)[c]	Chemical Formula as $[M-H]^-$	Calculated $[M-H]^-$ *m/z*	$[M-CO_2-H]^-$ [d] *m/z*	Epo-AnA as $[epoM-H]^-$	Relative abundance (%)[f]	RT (min)[c]	Calculated $[epoM-H]^-$ *m/z*	$[epoM-CO_2-H]^-$ [d] *m/z*	Double bond location [e]	
											~~D~~ Δ	~~w~~ ω
1	**13:0**	36.5	$[C_{20}H_{31}O_3]^-$	319.2279	275.2380	-	-	-	-	-	-	-
2	13:1	33.3	$[C_{20}H_{29}O_3]^-$	317.2122	273.2224	$[C_{20}H_{29}O_4]^-$	-	22.4	333.2071	289.2173	Δ^{4}	ω^{9}
3	**15:0**	41.0	$[C_{22}H_{35}O_3]^-$	347.2592	303.2693	-	-	-	-	-	-	-
4	15:1	36.7	$[C_{22}H_{33}O_3]^-$	345.2435	301.2537	$[C_{22}H_{33}O_4]^-$	100 [f]	27.8	361.2384	317.2486	Δ^{8} [g]	ω^{7}
5	15:1	36.7	$[C_{22}H_{33}O_3]^-$	345.2435	301.2537	$[C_{22}H_{33}O_4]^-$	40	28.9	361.2384	317.2486	Δ^{6}	ω^{9}
6	17:0	45.6	$[C_{24}H_{39}O_3]^-$	375.2905	331.3006	-		-	-	-	-	-
7	17:1	42.4	$[C_{24}H_{37}O_3]^-$	373.2748	329.2850	$[C_{24}H_{37}O_4]^-$	5 [f]	33.9	389.2697	345.2799	Δ^{10}	ω^{7}
8	**17:1**	42.4	$[C_{24}H_{37}O_3]^-$	373.2748	329.2850	$[C_{24}H_{37}O_4]^-$	100	34.6	389.2697	345.2799	Δ^{8}	ω^{9}
9	17:2	39.7	$[C_{24}H_{35}O_3]^-$	371.2592	327.2693	$[C_{24}H_{35}O_5]^-$	-	22.8	403.2490	359.2592	$\Delta^{8,11}$ [h]	$\omega^{6,9}$
10	17:3	37.6	$[C_{24}H_{33}O_3]^-$	369.2435	325.2537	$[C_{24}H_{33}O_6]^-$	-	6.4	417.2283	373.2384	$\Delta^{8,11,14}$	$\omega^{3,6,9}$
11	19:0	50.2	$[C_{26}H_{43}O_3]^-$	403.3218	359.3319	-	-	-	-	-	-	-
12	19:1	47.1	$[C_{26}H_{41}O_3]^-$	401.3061	357.3163	$[C_{26}H_{41}O_4]^-$	-	38.5	417.3010	373.3112	Δ^{10}	ω^{9}

[a] The phenolic lipid nomenclature of the delta (Δ) position was adopted in the present work to distinguish the double bond(s) in the alkyl chain. [b] Anacardic acids (*i.e.*, 2-hydroxy-6-alkyl-benzoic acids) are indicated with C carbon atoms in the side chain and N number of C-C double bonds after a colon (C:N); the most abundant species are reported in bold. [c] A C30 core-shell 2.6 µm column was used with a dead time of 1.75 min at a flow rate of 0.200 mL/min and 40 °C. [d] Decarboxylated and deprotonated AnAs. [e] Both shorthand nomenclatures, Δ and ω, were inserted for comparison with previous works: Δ is the position of the first double bond counted from the 6th position of benzene in 2-hydroxybenzoic acid; the nomenclature is called omega when the carbons are counted from the methyl end of the fatty alkyl chain. [f] The relative contents of these unsaturated AnAs were obtained from areas of epoxidated species, $[epoM-H]^-$, and they compare the abundance between isomers. [g] The common name of this *cis*-monounsaturated AnA 15:1D^{8} is ginkolic acid (Borenstein et al., 2020). [h] Merulinic acid C is the trivial name of AnA 17:2 D^{8,11} (Rodrigues-Costa et al., 2020).

Captions of Figures

Figure 1. Multiple EIC chromatograms obtained by RPLC-ESI-MS in the negative-ion mode of AnAs occurring in pistachio shell extracts: (A) AnAs 13:0 and 13:1, (B) 15:0 and 15:1, (C) 17:0, 17:1, 17:2, and 17:3. In each plot, the *m/z* ratios and the chemical formula of AnAs are given. A C30 column (core-shell 2.6 µm) operating at 40 °C was used.

Figure 2. Triple-stage CID (MS^3) spectra of the following decarboxylated AnAs: (A) 17:0 at *m/z* 331.3, (B) 17:1 at *m/z* 329.3, (C) 17:2 at *m/z* 327.3, and (D) 17:3 at *m/z* 325.3. Product ions at *m/z* 106.0, 107.0, and 119.0 are typical peak signals observed in the MS^3 spectra of AnAs. No diagnostic product ions for C=C location(s) were detected.

Figure 3. Multiple EIC chromatograms resulting from RPLC-ESI-MS with a C30 column of epoxidized AnAs obtained upon epoxidation reaction of a sample extracted from pistachio-dried shells. Chromatographic profiles correspond to: (A) epo-AnAs 13:1, 15:1 and 17:1, and (B) epo^2-AnAs 17:2 and epo^3-AnAs 17:3. Column temperature, 40 °C.

Figure 4. ESI(−)-CID-MS/MS product ion spectra of deprotonated epo-AnAs 17:1 and 15:1: (A)/(B) spectra for precursor ions at *m/z* 389.3, corresponding to epo-AnA 17:1 isomers eluting at 34.6 and 33.9 min, respectively. (C)/(D) spectra for precursor ions at *m/z* 361.2, corresponding to epo-AnA 17:1 isomers eluting at 27.8 and 28.9 min, respectively.

Figure 5. Suggested structures for product ions generated by CID-MS/MS of the standard AnA 15:3 $\Delta^{8,11,14}$. Diagnostic product ions for the assessment of the location of double C-C bonds are reported in bold.

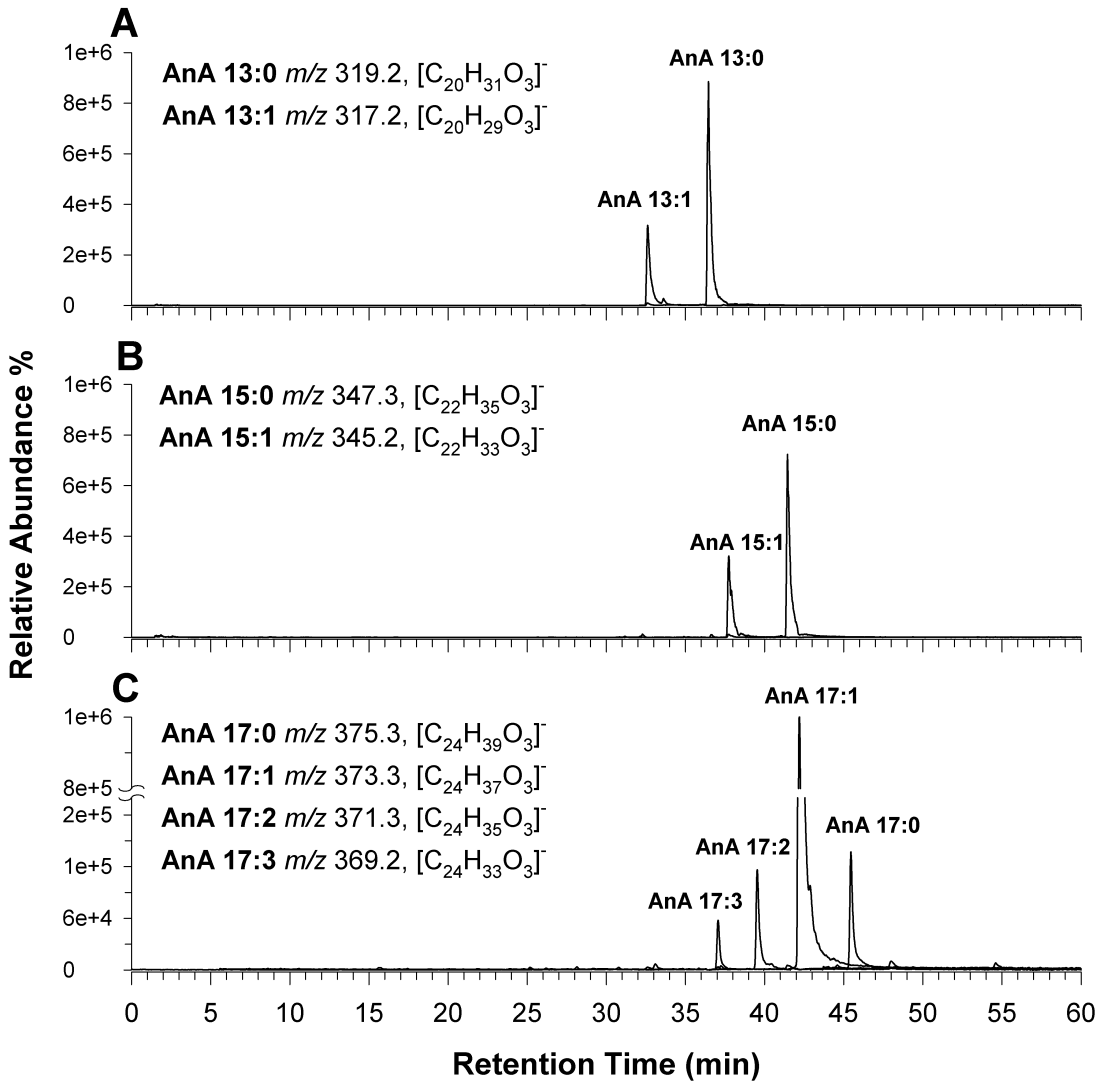
A
AnA 13:0 m/z 319.2, [C20H31O3]-
AnA 13:1 m/z 317.2, [C20H29O3]-
AnA 13:0
AnA 13:1
B
AnA 15:0 m/z 347.3, [C22H35O3]-
AnA 15:1 m/z 345.2, [C22H33O3]-
AnA 15:0
AnA 15:1
C
AnA 17:0 m/z 375.3, [C24H39O3]-
AnA 17:1 m/z 373.3, [C24H37O3]-
AnA 17:2 m/z 371.3, [C24H35O3]-
AnA 17:3 m/z 369.2, [C24H33O3]-
AnA 17:1
AnA 17:0
AnA 17:2
AnA 17:3
Relative Abundance %
Retention Time (min)

Figure 1.

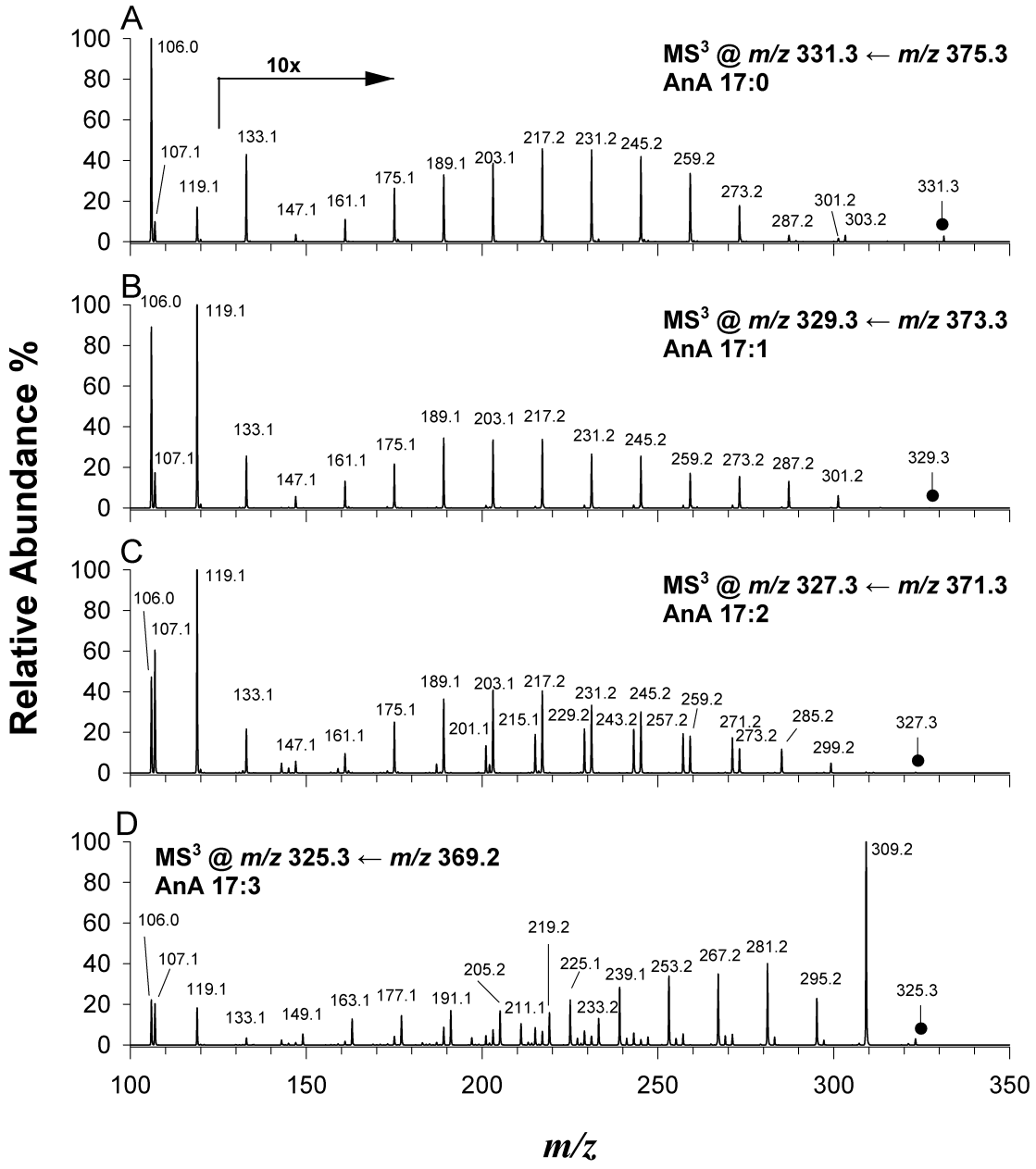
A
MS3 @ m/z 331.3 ← m/z 375.3
AnA 17:0
10x
106.0
107.1
119.1
133.1
147.1
161.1
175.1
189.1
203.1
217.2
231.2
245.2
259.2
273.2
287.2
301.2
303.2
331.3
B
MS3 @ m/z 329.3 ← m/z 373.3
AnA 17:1
106.0
107.1
119.1
133.1
147.1
161.1
175.1
189.1
203.1
217.2
231.2
245.2
259.2
273.2
287.2
301.2
329.3
C
MS3 @ m/z 327.3 ← m/z 371.3
AnA 17:2
106.0
107.1
119.1
133.1
147.1
161.1
175.1
189.1
201.1
203.1
215.1
217.2
229.2
231.2
243.2
245.2
257.2
259.2
271.2
273.2
285.2
299.2
327.3
D
MS3 @ m/z 325.3 ← m/z 369.2
AnA 17:3
106.0
107.1
119.1
133.1
149.1
163.1
177.1
191.1
205.2
211.1
219.2
225.1
233.2
239.1
253.2
267.2
281.2
295.2
309.2
325.3
Relative Abundance %
m/z
0
20
40
60
80
100
100
150
200
250
300
350

Figure 2.

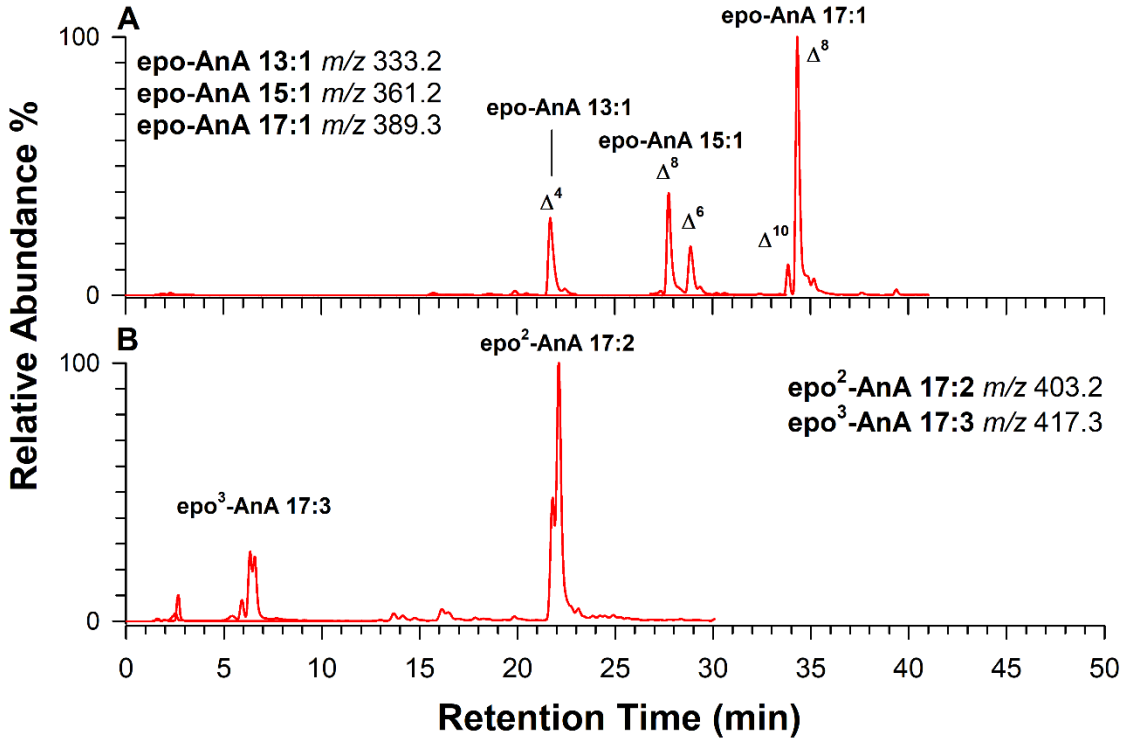
A
epo-AnA 13:1 m/z 333.2
epo-AnA 15:1 m/z 361.2
epo-AnA 17:1 m/z 389.3
epo-AnA 13:1
epo-AnA 15:1
epo-AnA 17:1
Δ4
Δ8
Δ6
Δ10
Δ8
B
epo2-AnA 17:2
epo3-AnA 17:3
epo2-AnA 17:2 m/z 403.2
epo3-AnA 17:3 m/z 417.3
Relative Abundance %
100
0
100
0
0
5
10
15
20
25
30
35
40
45
50
Retention Time (min)

Figure 3.

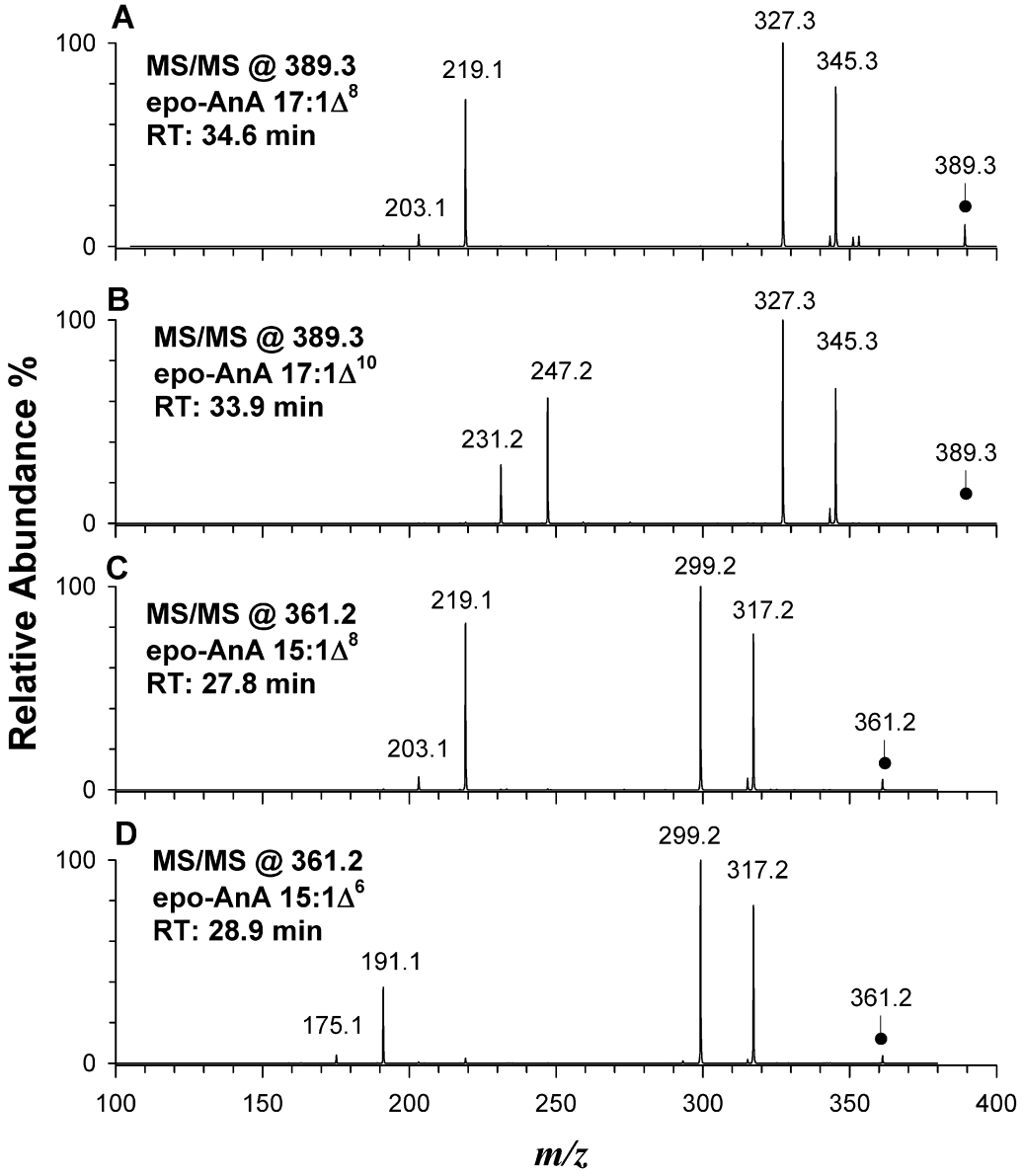
A
MS/MS @ 389.3
epo-AnA 17:1Δ8
RT: 34.6 min
B
MS/MS @ 389.3
epo-AnA 17:1Δ10
RT: 33.9 min
C
MS/MS @ 361.2
epo-AnA 15:1Δ8
RT: 27.8 min
D
MS/MS @ 361.2
epo-AnA 15:1Δ6
RT: 28.9 min
Relative Abundance %
m/z

Figure 4.

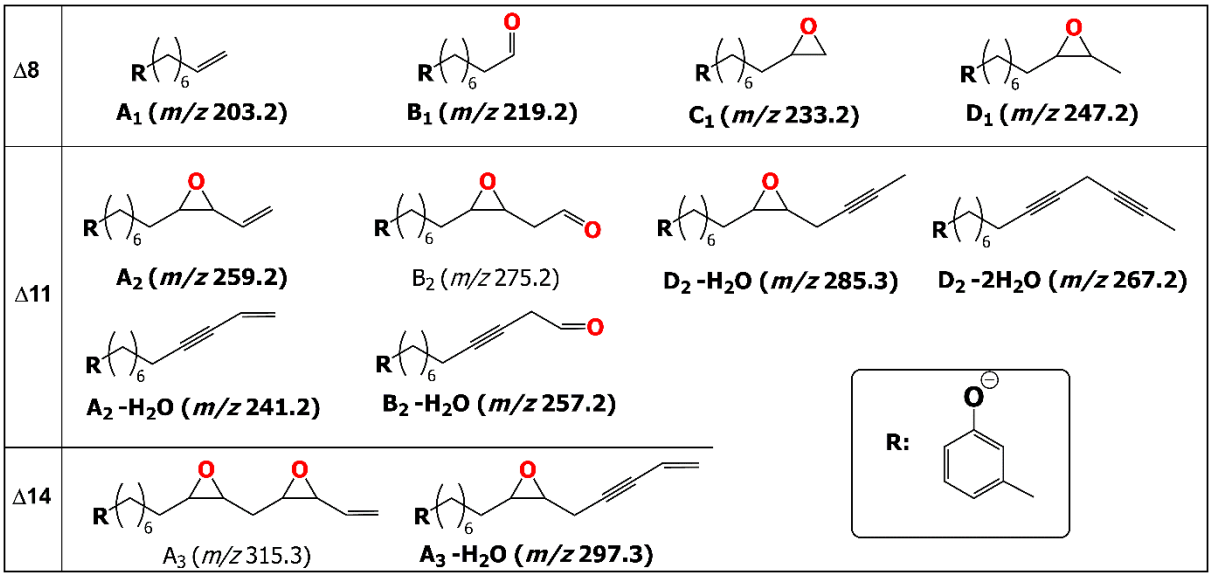
Δ8
A1 (m/z 203.2)
B1 (m/z 219.2)
C1 (m/z 233.2)
D1 (m/z 247.2)
Δ11
A2 (m/z 259.2)
B2 (m/z 275.2)
D2 -H2O (m/z 285.3)
D2 -2H2O (m/z 267.2)
A2 -H2O (m/z 241.2)
B2 -H2O (m/z 257.2)
R:
Δ14
A3 (m/z 315.3)
A3 -H2O (m/z 297.3)

Figure 5.